

EXPLOITING AMBIENT NOISE FOR SOURCE CHARACTERIZATION OF REGIONAL SEISMIC EVENTS

Michael H. Ritzwoller, Anatoli L. Levshin, and Mikhail P. Barmin

University of Colorado at Boulder

Sponsored by the National Nuclear Security Administration

Award No. DE-AC52-09NA29326

Proposal No. BAA09-52

ABSTRACT

The purpose of this research is to develop and test novel methods to characterize regional seismic events by exploiting Empirical Green's Functions (EGF) that are produced from ambient noise. Elastic EGFs between pairs of seismic stations are determined by cross-correlating long ambient noise time-series recorded at the two stations. The EGFs principally contain Rayleigh and Love wave energy and our focus is placed on utilizing these signals between periods of 5- and 15-sec. Epicentral location based on the envelope functions of the Rayleigh wave EGFs has been described by Barmin et al. (2011) and epicentral location based on the joint interpretation of observations of Rayleigh and Love wave group travel times has been described by Levshin et al. (2012). During the past year we have extended the method to incorporate phase travel times and to redefine the method to be based on phase and group velocity maps derived from ambient noise data rather than observations obtained directly on the EGFs. These refinements stabilize the location procedure and now allow us to estimate hypocentral depth and the source mechanism of regional events.

OBJECTIVES

The purpose of this research is to improve seismic event location accuracy and event characterization by exploiting Empirical Green's Functions (EGFs) that emerge by cross-correlating long time sequences of ambient noise observed at pairs of seismic stations. Because ambient noise EGFs are dominated by surface waves, the method uses surface wave energy for location purposes. The method of epicentral location as well as proof-of-concept applications to a set of seismic events in the western US have been described by Ritzwoller et al. (2009) and more recently and completely by Barmin et al. (2011) and Levshin et al. (2012) referred to here as Papers I and II. During the past year we have extended the method to incorporate phase travel times and to redefine the method to be based on phase and group velocity maps derived from ambient noise data (or a 3-D model based on ambient noise) rather than observations obtained directly on the EGFs. The use of group and phase time residuals for estimating source mechanism and depth was investigated using USArray Transportable Array (TA) data and reveals encouraging results.

RESEARCH ACCOMPLISHED

1. Introduction

The purpose of this work is to investigate how ambient noise can be used to improve regional to local scale event characterization. Ambient noise cross-correlations provide new information about crustal structure revealed dominantly through Rayleigh and Love waves. The cross-correlations themselves, group or phase velocity maps determined from them, or 3-D crustal and uppermost mantle models determined from them can be exploited to improve estimates of epicentral location and, in principal, also focal mechanism and hypocentral depth for seismic sources larger than magnitude 3.0-3.5.

Barmin et al. (2011), referred to hereafter as Paper I, presented a new approach to the epicentral location of shallow seismic events based on use of the Empirical Green's Functions (EGFs) obtained from ambient seismic noise. The vertical component of the ambient noise in the period range from 7 to 15 s, which is dominated by the fundamental Rayleigh wave, was used to compute the EGFs. It was demonstrated that this approach has several features that make it a useful addition to existing location methods. First, the method is based on surface waves, which are usually not applied in most location algorithms. Second, it does not require knowledge of Earth structure

and is, therefore, unbiased by uncertainties in the knowledge of structure near the epicenter. Third, it works well for weak seismic events even if the detection of body wave phases is problematic. Fourth, the EGFs computed during a temporary deployment of a base network (such as the USArray Transportable Array (TA) or PASSCAL deployments) may be applied to events that occur earlier or later using permanent remote stations even if the temporary stations are absent.

The method presented in Paper I has several limitations. In particular, it is based on the assumption that the event source mechanism and depth are unknown and does not attempt to estimate them. Time shifts in the surface waves caused by the source mechanism, therefore, can bias the epicentral location. Paper I shows that this degradation is worst for source depths between about 2 and 5 km if the source mechanism is different from pure strike-slip, thrust or normal faulting. In this case, the method described in Paper I will deliver a biased estimate of the epicentral location.

Levshin et al. (2012), hereafter referred to as Paper II, addressed this limitation by introducing Love waves into the location method. Love waves possess different sensitivity to the source mechanism than Rayleigh waves and, in fact, Love wave source phase times are quantitatively less sensitive to the source mechanism (Levshin et al., 1999). Love waves are, however, in many cases more difficult to observe than Rayleigh waves due to higher noise levels on horizontal components. Epicentral estimates based on Love waves, therefore, have a larger variance than those based on Rayleigh waves, on average. Thus, the joint application of Rayleigh and Love waves to estimate epicentral locations may be preferable to the locations based on either wave type alone, as it strikes a balance between bias and variance.

The procedure presented in Paper II differs from that in Paper I in another way in addition to introducing Love waves. The direct comparison of envelope functions of the earthquake and ambient noise EGFs is replaced with comparing theoretical group velocity curves (computed, for example, from the EGFs, existing group velocity maps or a 3-D model) with the measured group velocity curves obtained from the event records. Using curves from existing group (or phase) velocity maps computed from ambient noise tomography or from curves predicted from a 3-D model that originated by inverting ambient noise dispersion maps, in particular, makes the algorithm more flexible and opens the possibility to estimate other source parameters such as hypocentral depth and the moment tensor.

Here we, first, summarize some of the principal results from Paper II, illustrating the effect of introducing Love waves with Rayleigh waves in a joint inversion for epicentral location. Second, we present some early results that demonstrate the feasibility of obtaining improved estimates of focal mechanism and depth based on using a 3-D model constructed from ambient noise.

2. Joint application of Rayleigh and Love wave EGFs to locate several events in the Western USA

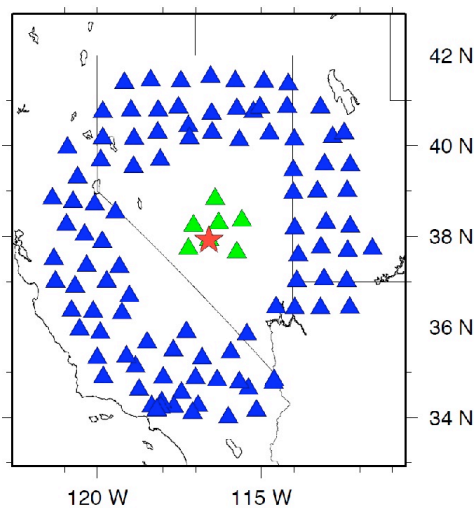


Figure 1. The network of base (green triangles) and remote (blue triangles) stations used in the synthetic location experiment from Paper II.

To clarify the capabilities of the methods described in Papers I and II we present examples of epicentral location using simulated seismograms for a set of theoretical earthquakes with different source mechanisms and depths located in central Nevada. **Figure 1** presents the locations of the base and remote stations used in the simulation. Synthetic seismograms and Green's functions (replacing the ambient noise EGFs) are computed for each theoretical earthquake and the location procedures in Papers I and II is applied. Examples of misfit surfaces using Rayleigh and Love waves, respectively, are presented in **Figure 2a,b** for the red focal mechanism shown in **Figure 3** at 5 km depth. This earthquake type and depth are chosen because they provide large Rayleigh wave group time shifts, which results in a large epicentral bias using Rayleigh waves alone as can be seen in **Figure 2a**.

In **Figure 2a**, the Rayleigh wave location is biased by about 2.0 km. In contrast, for this event there is very low bias using Love waves alone, as **Figure 2b** illustrates. Weighting Love waves and Rayleigh waves equally in the location algorithm, reduces the bias appreciably, although bias does remain at about 1.0 km, as seen in **Figure 2c**. However, if the wave types are weighted inversely by minimum misfit, which is very low for Love waves and considerably larger for Rayleigh waves, then the resulting joint location is again essentially unbiased, as **Figure 2d** shows.

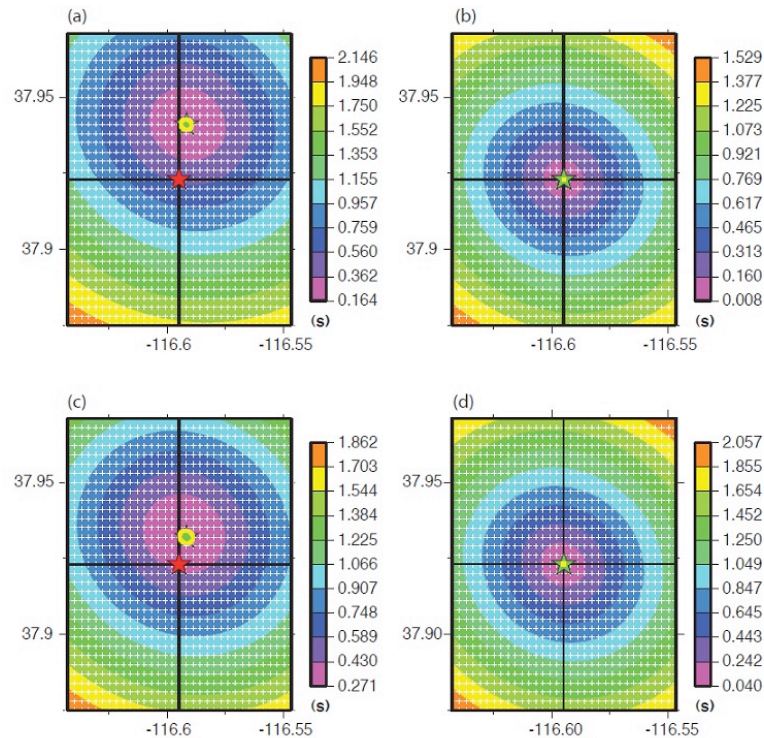


Figure 2. Simulated misfit for the virtual source whose location is shown in **Fig. 1** at 5 km depth and with red source mechanism shown in **Fig. 3**. Grid spacing is about 300 m. (a) Rayleigh wave location. (b) Love wave location. (c) Joint location where Rayleigh and Love waves are weighted equally. (d) Joint location where Love and Rayleigh waves are weighted by their minimum misfits.

We repeat this procedure systematically to estimate location bias for the four different mechanisms (red, green, light blue, dark blue) shown in **Figure 3** that occur at depths ranging from 1 to 25 km and with different data (Rayleigh, Love, joint) applied in the location procedure. Estimated bias using Rayleigh waves alone is shown in **Figure 3a**, using Love waves alone is shown in **Figure 3b**, using equally weighted Rayleigh and Love waves jointly is shown in **Figure 3c**, and using Rayleigh and Love waves jointly but weighted by minimum misfit is shown in **Figure 3d**. **Figure 3a** is similar to a result presented in Paper I, illustrating that location bias for Rayleigh waves can be large, up to several km, for certain types of events that occur between depths of 2 and 5 km. (This figure differs slightly from the comparable figure in Paper I in which large epicentral shifts more than 3 km from the input location were not considered and Paper I, therefore, slightly underestimated the level of bias.) **Figure 3b** illustrates that locations based on Love waves suffer a much smaller bias, with expected values less than about 400 m. Jointly interpreting equally weighted Rayleigh and Love waves reduces the Rayleigh wave bias substantially, but residual

bias at an expected level of about 1 km would remain for events between 2 and 5 km depth as Figure 3c shows. Finally, the location bias based on the joint location that differentially weights Rayleigh and Love waves inversely by misfit illustrates that the resulting bias is very low (Fig. 3d).

Bias is even lower than for Love waves alone because the effect of including the Rayleigh wave is to cancel part of the Love wave bias. It is tempting to conclude from these synthetic experiments that differentially weighting Rayleigh and Love waves based on minimum misfit would produce a largely unbiased estimator. This is true for noise-free data, but for real data the signal-to-noise ratio (SNR) of Love waves is typically lower than of Rayleigh waves and the minimum Love wave misfit is not much lower than the Rayleigh wave misfit even in the best cases. In fact, on average, Love wave misfit is higher than for Rayleigh waves. In practice, it is difficult with real data to identify the events for which the Rayleigh wave location would be biased. Although misfit is an excellent guide for synthetic data, for real data it is at best imperfect. For this reason, in presenting results with real data below we will only show joint locations that weight Rayleigh and Love waves equally. A better scheme may be found for particular applications, however.

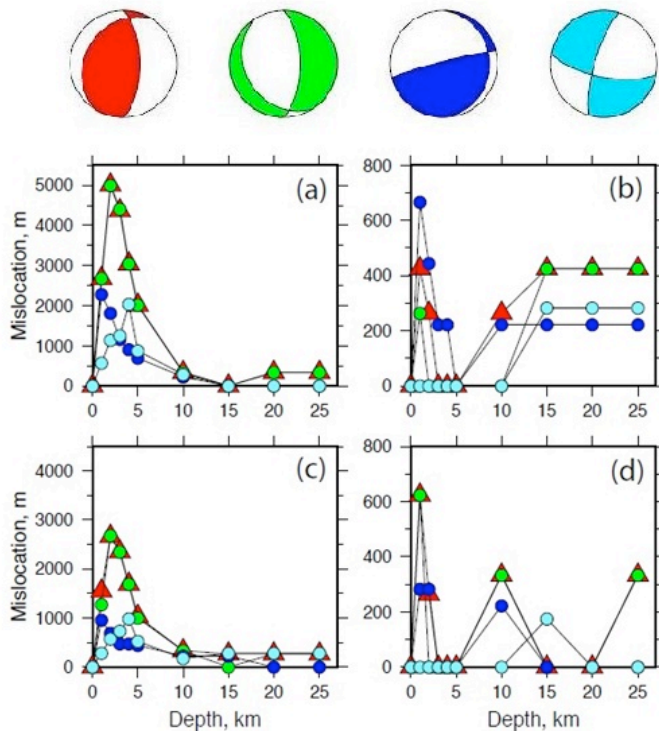


Figure 3. Summary of the mislocations found in the synthetic experiment as a function of the source depth for the four source mechanisms shown at top: red, green, dark blue, light blue. In (a) Rayleigh waves are used alone, in (b) Love waves are used alone, and in (c) Rayleigh and Love waves are used jointly and weighted identically. In (d) Rayleigh and Love waves are used jointly and weighted inversely by the minimum misfit for each wave type (with weights 0.95 and 0.05, correspondingly).

To test the ability of joint use of Rayleigh and Love wave EGFs to locate earthquakes and mining events, we selected Ground Truth events with magnitudes in the 3s or 4s whose epicenters and depths are well known, in particular with epicenters known to 500 m or better. Such events are strikingly rare in the western US. These include the Crandall Canyon Mine collapse in Utah on August 6, 2007 (Pechmann et al., 2007) whose location using Rayleigh wave EGFs was described in Paper I, two Ground Truth events in California and Utah, the Wells earthquake in Western Nevada, and the sequence of its aftershocks (Mendoza & Hartzell, 2009).

Results of locations are summarized in Table 1. The deviations of our locations from references are mostly less than 1.5 km for any combination of Rayleigh or Love waves. It is necessary to take into account that the accuracy of reference locations is mostly not better than 1 km and in the case of Wells events may be worse. The distances between locations using Rayleigh and Love EGFs vary between 0 and 2.3 km and on average are less than 1.1 km. Error ellipses for the 95% confidence level obtained for Rayleigh (*R*), Love (*L*), and joint (*RL*) locations cover the reference locations and mostly overlap each other as Figures 4 and 5 illustrate. The size of the error ellipses for Love wave locations is comparable or slightly larger than for Rayleigh waves. Ellipses for joint Rayleigh and Love wave locations are mostly the smallest among the three types of location procedures.

Table 1. Locations using Rayleigh (R) waves, Love waves (L), and both waves (RL).

Event	Ref-R, km	Ref-L km	Ref-RL km	RMS_Q s	Q	Ellipse km	Q
Earthquake, CA	0.7	1.9	0.7	1.2	R	2.5	RL
Mine collapse, UT	0.4	0.7	0.7	1.4	R	1.4	RL
Earthquake, UT	1.3	0.0	0.4	0.9	R	1.7	RL
Wells Event, NV	0.6	1.1	0.6	0.7	R	1.1	R
aftershock#1	0.7	0.7	0.7	0.7	R	0.9	RL
aftershock#2	0.4	0.6	0.4	1.0	R	1.4	R
aftershock#3	1.1	0.7	0.7	0.7	R	0.8	RL
aftershock#4	0.0	1.0	0.7	0.8	L	1.0	RL
aftershock#5	1.2	1.4	1.2	0.8	L	1.0	RL
aftershock#6	0.4	1.2	0.7	0.6	R	1.1	RL

“Ref-R” is the distance between the reference (GT) location and the Rayleigh wave location. “Ref-L” is the same but for Love waves. “Ref-RL” is the same but using both types of waves. “Misfit” is the minimum value (sec) of the misfit functionals F_R , F_L , and F_{RL} . “Ellipse” is the length (km) of the semi-major axis of the 95% confidence ellipse. Epicentral grid spacing is 500m for earthquakes and 200m for the Utah mine collapse. “Q” specifies which method produces the best result: Rayleigh wave location (R), Love wave location (L), or joint location using both wave types weighted equally (RL).

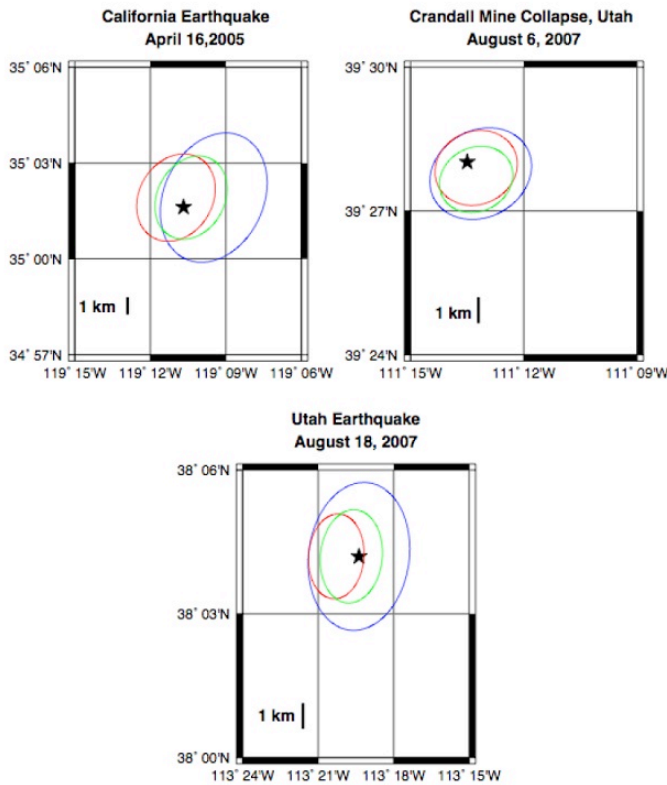


Figure 4. Locations of reference events (stars, Table 1) in California and Utah compared with locations from the methods described herein. Ellipses correspond to the 95% confidence level where the location results from the Rayleigh estimator (red ellipse), the Love estimator (blue ellipse), and the joint estimator where Rayleigh and Love waves are equally weighted (green ellipse).

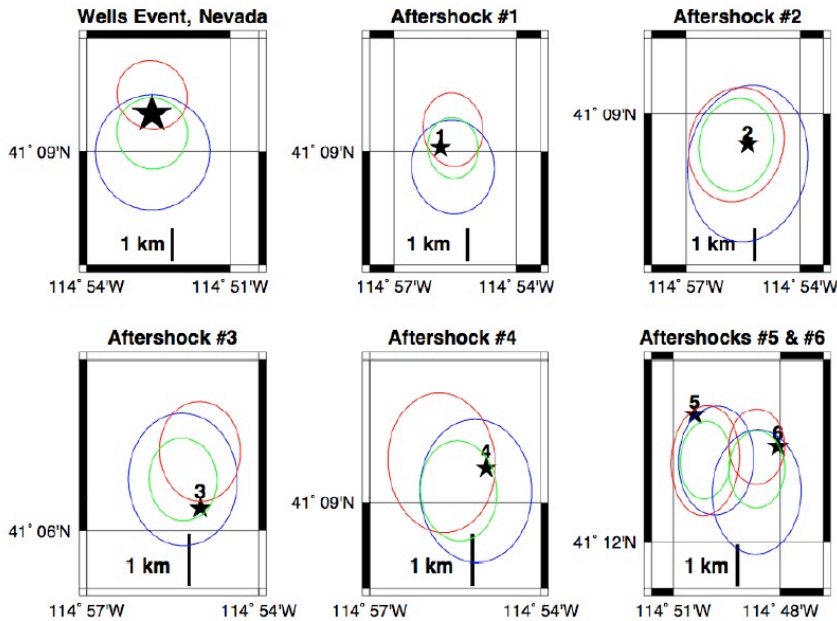


Figure 5. Same as Fig. 4, but for the location of the large Wells earthquake on 21 February 21 2008 and its six aftershocks.

3. Source characterization based on travel times from a 3-D model estimated from ambient noise

The methods described above and in Papers I and II are designed to estimate epicentral location based either on comparison of the envelopes of the event waveform with ambient noise empirical Green's functions or on group times measured from ambient noise EGFs and event waveforms. There are two primary shortcomings of the method. First, the method only provides information about epicenter and not focal mechanism, moment, or hypocentral depth. Second, there is data other than group times that can be used to constrain other aspects of the source and, in fact, group times are a difficult observable compared with phase times. The other data includes both Rayleigh and Love wave phase travel times for the fundamental mode as well as the spectral amplitudes of the Rayleigh and Love waves.

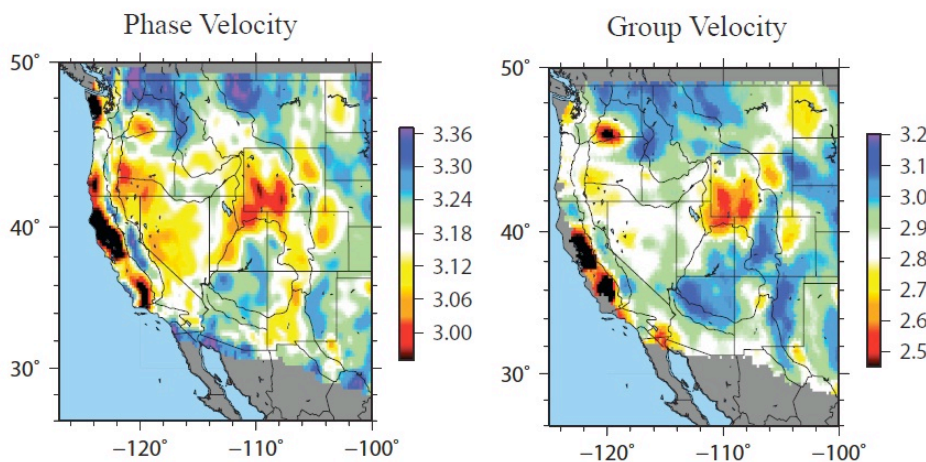


Figure 6. Rayleigh wave phase and group velocity maps at 10 s period predicted from the 3-D model of Shen et al. (2012).

Ambient noise tomography provides ideal information to construct maps of phase and group speeds across extended regions and 3-D models of V_s in the crust and uppermost mantle. The US is the best region for this application because of the USArray Transportable Array (e.g., Fig. 6), but countries on other continents increasingly

have been developing extended seismic networks of hundreds to thousands of broadband seismometers that can be used to produce similar models (e.g., China, Europe). Increasingly accurate azimuthally anisotropic maps are also becoming available as seen in [Figure 7](#).

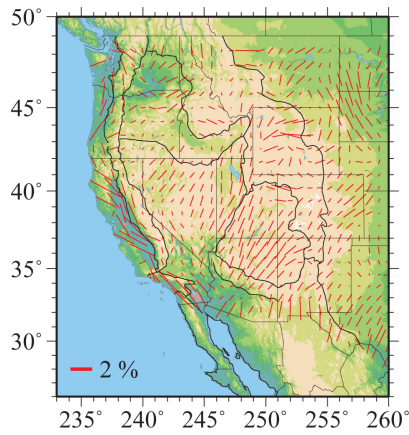


Figure 7. The map of 2ψ -anisotropy for Rayleigh wave phase velocity in percent at 10 s period.

The quality of source characterization will depend in large part on the ability to predict observables without bias using an earth model. 1-D models notoriously produce biased location estimates as the number of observing stations reduces and as open azimuth increases. Misfit information using a 1-D model following one of the Wells aftershocks in northeastern Nevada is shown in [Figure 8](#).

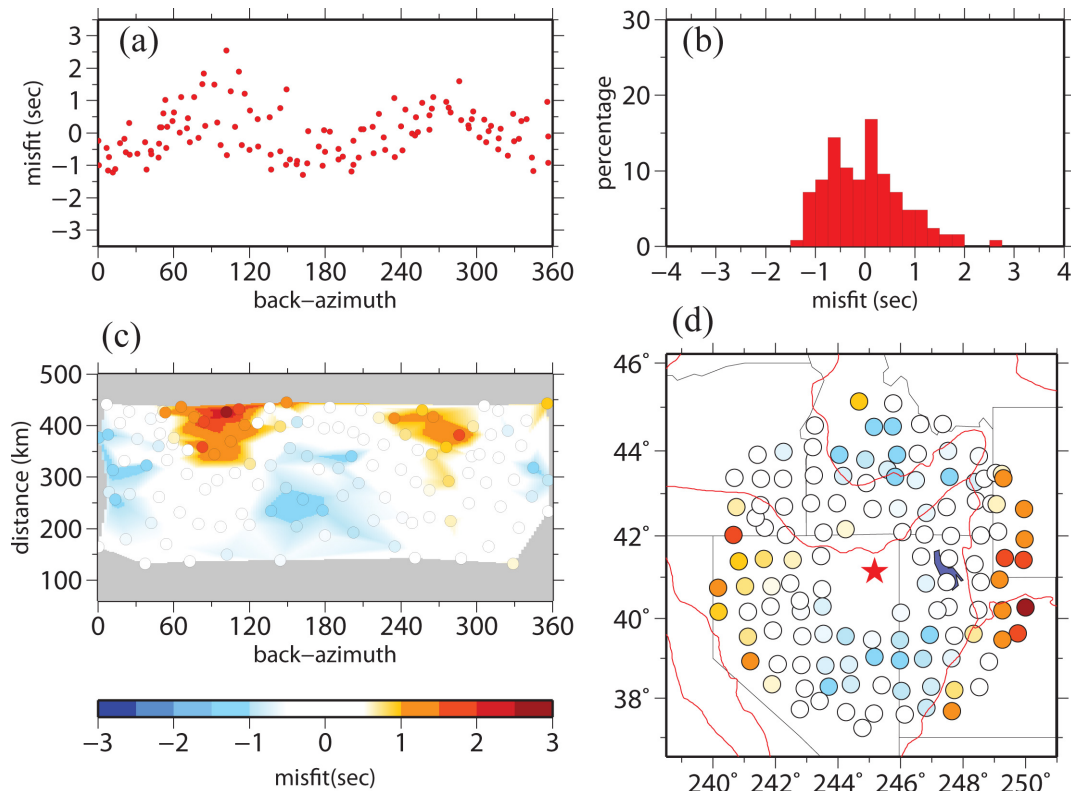


Figure 8. Summary of misfit to observations of phase travel time at 12 sec period observed after the Wells aftershock #4 (Feb 28 2008, $M=3.9$) using an average 1-D model for the region after correcting for source mechanism. (a) Misfit at individual stations plotted as a function of azimuth ($N=0^\circ$, $E=90^\circ$, etc.). (b) Histogram of misfit (RMS misfit = 0.92 s). (c) Color-coded misfit plotted as a function of back-azimuth and distance. (d) Color-codes misfit plotted at station locations.

In contrast, an accurate 3-D model allows phase travel times to be fit much more accurately, as [Figure 9](#) illustrates. This will allow better epicentral location estimates based on phase travel times as well as provide better

estimates of focal mechanism. The inclusion of azimuthal anisotropy actually provides a significant component of the misfit improvement shown in Figure 9.

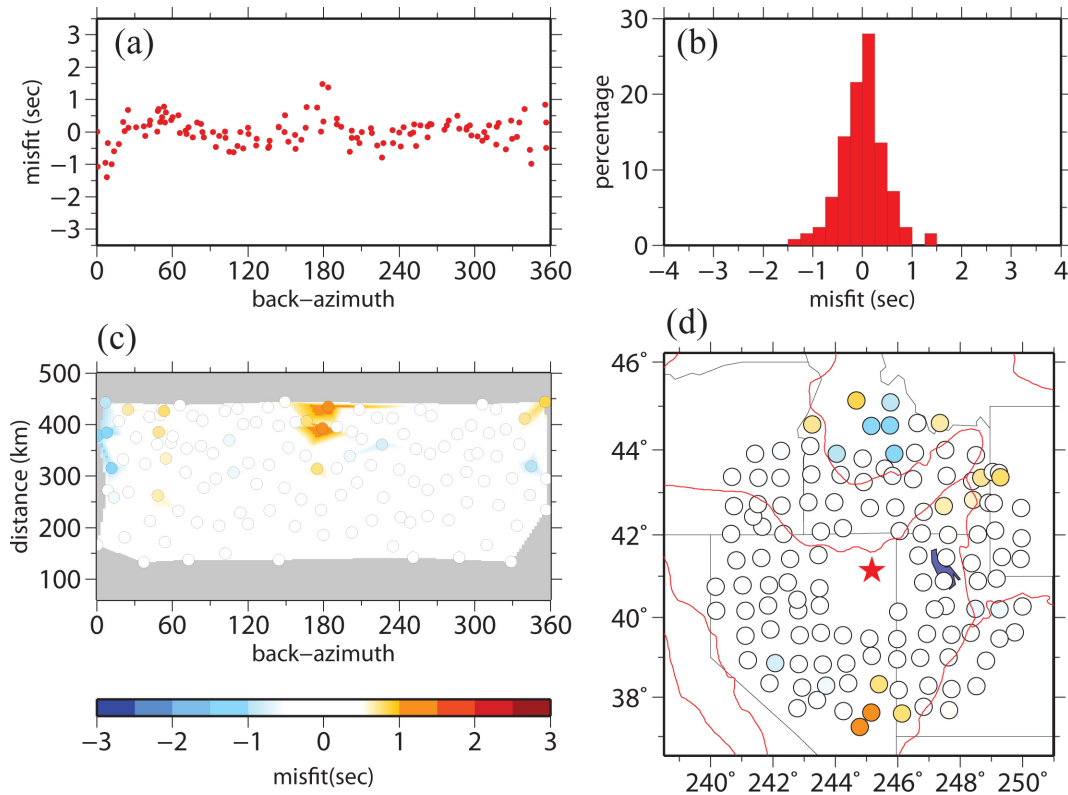


Figure 9. Same as Fig. 8, but computed from the 3-D isotropic model of Shen et al. (2012) with the azimuthal anisotropy from Lin et al. (2011). RMS misfit = 0.44s.

The region surrounding Wells, Nevada in the Basin and Range province is actually relatively homogeneous compared with most seismogenic regions. A better estimate of the advantage in fitting Rayleigh wave phase travel times using the 3-D model compared to a 1-D model is presented in Figure 10 for an earthquake near Dillon Montana in 2007 where the observing stations (USArray Transportable Array) were mainly to the west of the epicenter.

We have also estimated the ability of the 1-D and 3-D models to locate the Dillon, MT earthquake from 2007. We do this by using random selections of 5-station subsets of the TA network. Fixing the focal mechanism and depth estimated with the 3-D model using the full observing network (>100 stations) and using the epicenter determined from the full network based on the 3-D model as a reference, we randomly generated 5-station subsets of the full network and located the epicenter based on Rayleigh wave travel times alone at 12 sec period. Using the 1-D model we found that there was an rms error in the epicentral location of about 7.0 km with a 3.9 km bias. With the 3-D model, in contrast, we found that the rms error in the epicenter reduced to about 2.0 km with a 0.5 km bias. Thus, with a small number of stations and a far from ideal observing geometry, the 3-D model produced nearly unbiased epicentral location with an uncertainty of about 2 km, an improvement of more than a factor of three relative to the 1-D model in random error and a factor of eight in systematic error.

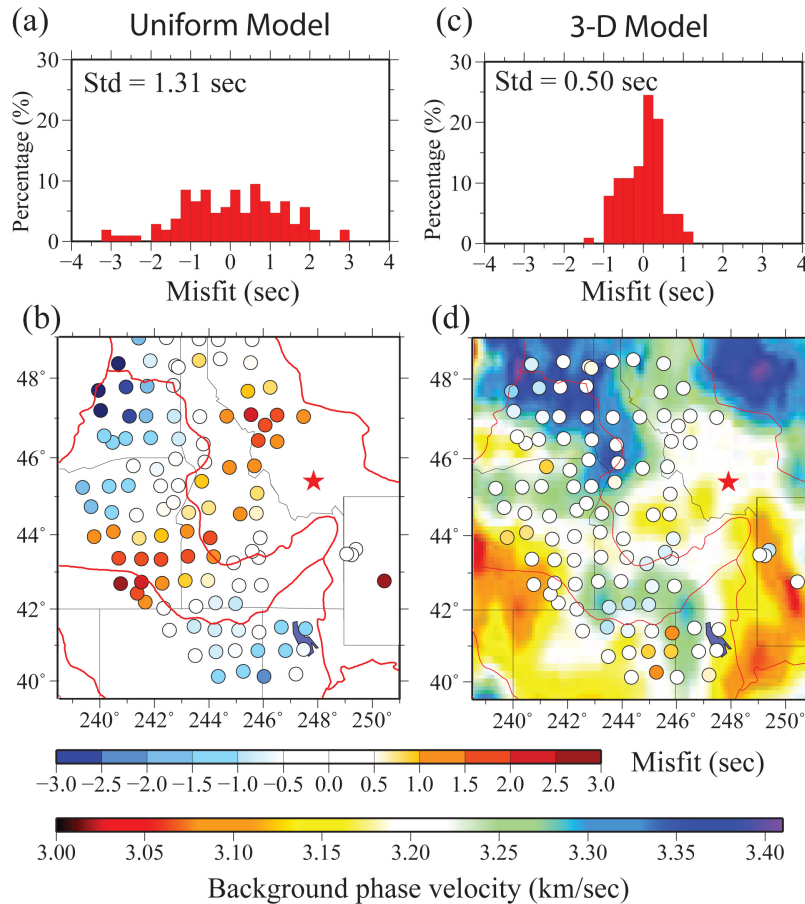


Figure 10. Comparison of misfit to Rayleigh wave phase travel time measurements at 12 sec period using (a,b) a laterally uniform model taken from the 3-D model of Shen et al. (2012) at the epicentral location and (c,d,) the 3-D model of Shen et al. (2012b). Earthquake (red star in (b), (d)): 2007/05/08 15:46:49 45.394N 112.130W, M=4.5, Dillon Montana. In (b) and (d), misfit between +/-3 sec is color-coded in circles at each TA station (operating mostly to the west of the event) and model phase velocity is shown in the background.

Further applications are needed to definitively quantify the expected improvement in source characterization from a 3-D model based on ambient noise tomography. The use of Love waves and a broader period band (e.g., 8-14 sec rather than just 12 sec) should improve location capabilities beyond the examples that we present here. Based on phase travel times alone (perhaps augmented with group travel times), however, depth cannot be well estimated. To estimate depth spectral amplitudes need to be measured. Examples of observed spectral amplitudes corrected for geometrical spreading and average attenuation at 8 sec and 14 sec period for the Wells earthquake #4 are shown in Figure 11a. The scatter at 8 sec period is larger than at 14 sec period even though the amplitude at 8 sec is higher. This is because of interference from microseismic noise for this small earthquake. The expected amplitudes predicted from the focal mechanism estimated using the phase travel time data at 10 km depth are plotted over the observations. The ratio of spectral amplitudes at 14 sec and 8 period provides a constraint on event depth. Figure 11b presents a histogram of the ratio of the amplitudes at 14 sec and 8 sec period taken from Figure 11a. The mean and mode of the distribution of the amplitude ratio are about that expected for an event at 10 km depth. Events at depths of 6 km and 14 km predict amplitude ratios that are either too small or too large, respectively, compared with the observations. The spectral amplitude ratio method is a promising technique to constrain event depths, but further work is on-going to improve measured spectra and to correct them for propagation effects such as attenuation, site response, and focusing/defocusing.

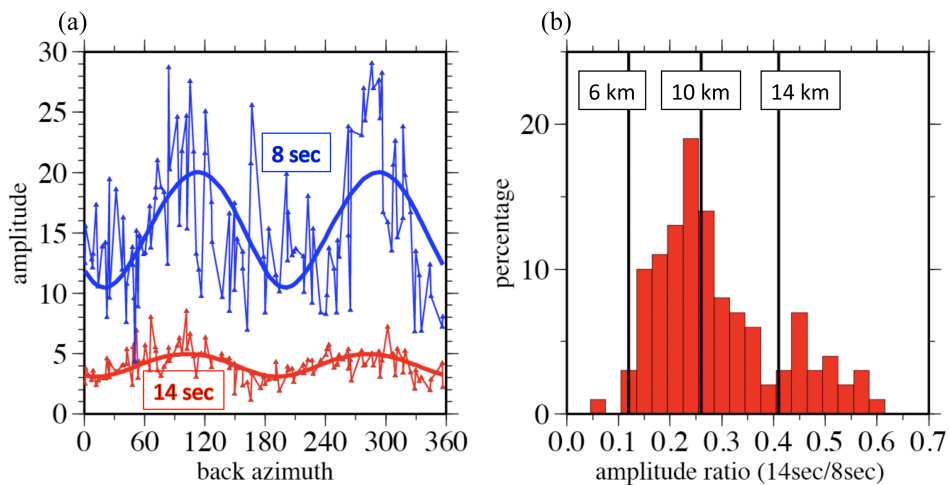


Figure 11. Example of the use of the ratio of Rayleigh wave amplitudes at different periods to estimate event depth for the Wells aftershock #4 ($M=3.9$). (a) Measured Rayleigh wave amplitudes as a function of azimuth corrected for geometrical spreading and average attenuation at 8 sec period (blue triangles) and 14 sec period (red triangles) observed at USArray TA stations at epicentral distances from 150 km and 450 km. Predicted curves are drawn with bold lines using a hypocentral depth of 10 km and the focal mechanism determined from phase travel times. (b) Histogram of the ratio of observed amplitudes in (a) at each azimuth. Black vertical lines indicate the expected value of the spectral ratios at 14 sec and 8 sec period for the event at different depths. A depth of 10 km agrees best with the observations in (a).

CONCLUSIONS AND RECOMMENDATIONS

The method to locate the epicenter of regional seismic events based on the envelope of Empirical Green's Functions determined from ambient seismic noise that has been described by Barmin et al. (2011) and Levshin et al. (2012) has several features that make it a useful addition to existing location methods. Love wave EGFs are less sensitive to unknown source parameters (moment tensor, depth) than Rayleigh EGFs and may provide smaller bias in location for source depths between 1 and 7 km. The advantage of using Love waves to locate seismic events is mitigated by the fact the Love wave EGFs typically have a lower SNR than Rayleigh waves, however. We demonstrate that the combined use of both types of waves provides locations with the smallest error ellipses. The next step in development of the method is based on using regional 3-D models obtained by tomographic inversion of ambient noise EGFs (e.g., Shen et al., 2012). Phase and group travel times predicted by these models are compared with observed travel times to estimate both epicentral location and focal mechanism. The results presented here illustrate that this technique can be used to improve location and focal mechanism for small crustal events. Depth can be constrained by measuring ratios of the amplitudes of Rayleigh waves at different periods, such as 14 sec and 8 sec period used here.

ACKNOWLEDGEMENTS

This research was supported by DoE/NNSA contract DE-AC52-09NA29326. The facilities of the IRIS Data Management System, and specifically the IRIS Data Management Center, were used to access the waveform and metadata required in this study. The IRIS DMS is funded by the National Science Foundation and specifically the GEO Directorate through the Instrumentation and Facilities Program of the National Science Foundation under Cooperative Agreement EAR-0552316. We are grateful to Drs. C. Mendoza and M.P. Moschetti for their help in data analysis and Dr. F.-C. Lin and Mr. W. Shen for providing us with Rayleigh wave phase and group velocity maps for the Western USA.

REFERENCES

Barmin, M.P., A.L. Levshin, Y. Yang, and M.H. Ritzwoller (2011). Epicentral location based on Rayleigh wave Empirical Green's Functions from ambient seismic noise, *Geophys. J. Int.*, **184**, 869-884, doi: 10.1111/j.1365-246X.2010.04879.x.

- Levshin, A.L., M.H. Ritzwoller, and J.S. Resovsky (1999). Source effects on surface wave group travel times and group velocity maps, *Phys. Earth Planet. Inter.*, **115**, 293-312.
- Levshin, A.L., M.P. Barmin, M.P. Moschetti, C. Mendoza, and M.H. Ritzwoller (2012). Refinements to the method of epicentral location based on surface waves from ambient seismic noise: Introducing Love waves, *Geophys. J. Int.*, (in press).
- Lin, F., M.H. Ritzwoller, Y. Yang, M.P. Moschetti, and M.J. Fouch (2011). Complex and variable crustal and uppermost mantle seismic anisotropy in the western United States, *Nature Geoscience*, DOI:10.1038/NGEO1036.
- Mendoza, C. and S. Hartzell (2009). Source analysis using regional empirical Green's functions: The 2008 Wells, Nevada, earthquake, *Geophys. Res. Lett.*, **36**, L11302, doi:10.1029/2009GL038073.
- Pechmann, J. C., W.I. Arabasz, K.L. Pankow, R. Burlacu, and M.K. McCarter (2007), Seismological report on the 6 Aug 2007 Crandall Canyon Mine Collapse in Utah, *Seismol. Res. Lett.*, **79**, 5, 620-636.
- Ritzwoller, M.H., M.P. Barmin, A.L. Levshin, and Y. Yang (2009). Epicentral location of regional seismic events based on empirical Green functions from ambient noise, in *Proceedings of the 31th Monitoring Research Review: Ground-Based Nuclear Explosion Monitoring Technologies*, LA-UR-09-05726, pp. 389-398.
- Shen, W., M.H. Ritzwoller, V. Schulte-Pelkum, F.-C. Lin (2012). A 3-D model of the crust and uppermost mantle beneath the central and western US by joint inversion of receiver functions and surface wave dispersion, *J. Geophys. Res.*, submitted.